Design and Modeling of a Dosing Unit in a Capsule-Filling Machine

Published Version:
Magri, F., Sciarra, G., Mottola, G., Lelli, G., Carricato, M. (2024). Design and Modeling of a Dosing Unit in a Capsule-Filling Machine. Cham : Springer Nature Switzerland AG [10.1007/978-3-031-64553-2_21].

Availability:
This version is available at: https://hdl.handle.net/11585/986694 since: 2025-07-28

Published:
DOI: http://doi.org/10.1007/978-3-031-64553-2_21

Design and modeling of a dosing unit in a capsule-filling machine

Filippo Magri, Giuseppe Sciarra, Giovanni Mottola, Gabriele Lelli and Marco Carricato

Abstract This paper focuses on the design of a dosing unit in an automatic machine to fill capsules with pellets. We first define the design requirements and constraints, such as the end-effector trajectory, the overall maximum dimensions, the adoption of low-lubrication systems to minimize contamination risk, architecture simplicity, and washability. Through an initial feasibility study, we select the solution that best satisfies the goals. The kinematic and dynamic model of the dosing unit is built and validated by a multibody simulation. The numerical model is used to construct an iterative process for sizing the motors and the unit inner mechanisms, to optimize dimensions, reduce peak accelerations, and achieve the desired transmission ratio. Finite-Element Analysis is finally performed for the most critical components. The new dosing group is capable of high-speed operation with optimal dosing accuracy.

Key words: Dosing Unit, Capsule-filling machine, Pellets, Slider-Crank Linkage, Optimization.

1 Introduction

Automatic capsule-filling machines are widely used by pharmaceutical companies to reduce production time and standardize the quality of products. Automated processes allow the production of high-quality tablets that comply with existing medical standards [1], like cGMP (*Current Good Manufacturing Practices*). The products are capsules that can contain tablets, micro tablets, granulates, powders, liquids and pellets. In a capsule-filling machine, the capsules are moved with an intermittent motion through several stations, each performing different tasks, such as capsule

Marco Carricato
University of Bologna, Viale Risorgimento 2, 40137 Bologna (BO), Italy, e-mail: marco.carricato@unibo.it

feeding, opening, closure, and unloading, together with product dosing, discarding unopened capsules, and cleaning the capsule containers.

In this paper, we focus on the design and modeling of a novel dosing unit for pellets. A dosing unit consists of a dosing head (DH) and its motion system [2, 3]. The DH includes dosing syringes, which create chambers of prescribed dimensions (by the motion of pistons) depending on the required dose of pellets. The work cycle starts with the dosing syringes immersed in the feeding tank. A vacuum system is activated, and the product is sucked inside the syringes. Then, the DH rises and moves horizontally towards the capsule filling area, where the product can be released from the syringes. The trajectory of the DH is shaped as an upside-down "L". Finally, the DH returns above the feeding tank and the cycle restarts. The system has thus 3 DoF: the horizontal and vertical translations of the DH, and the vertical translation of the syringes with respect to the DH. The current design is based on a serial mechanism composed by 3 active prismatic joints. Accordingly, two motors are not mounted on the frame, which significantly limits the operating speed. To guarantee washability and minimize the risk of contamination, pellets must be separated from mechanical components, which must be contained within one or more rubber bellows: the current design uses a single bellow that undergoes multi-axial deformations, which cause its rapid damage.

Based on known design approaches [4], we first identify different conceptual design solutions, which are ranked based on weighted design objectives. This process assists in selecting the most suitable solution. The design objectives of the group are flexibility, high speed (up to 140 cycles/min), zero leakage of lubricant, low lubrication requirements, washability, architecture simplicity, and reduced dimensions. All motors, mechanisms, and electronics must fit a parallelepiped housing with a 350×350 mm base and a 500 mm height. Rubber bellows must undergo axial deformations only, to improve their fatigue life. Rotary motors are to be preferred over linear ones, to maximize operating speed and precision, and to reduce costs.

In the final design, the DH includes a slider-crank linkage (SCL) that moves the pistons in the syringes to create the dosing chambers. Two other independent mechanisms control the motion of the DH: a four-bar parallelogram (FBP) joined with a SCL, for the vertical motion, and another SCL, for the horizontal motion. A kinematic and dynamic model of the dosing unit is developed in MATLAB and solved through an iterative procedure to find the optimal size for components and motors. The model is validated with a multibody simulation performed in CREO Mechanism. The transmission ratio of the SCL in the DH is optimized to minimize the ratio between the total piston stroke and the motor rotation, since this allows an accurate control of the dosing chamber dimensions. Critical components are finally analyzed by using Finite-Element Analysis (FEA).

This paper is organized as follows. Section 2 introduces the design approach. Section 3 presents the design of the dosing unit. Section 4 discusses conclusions and future work.

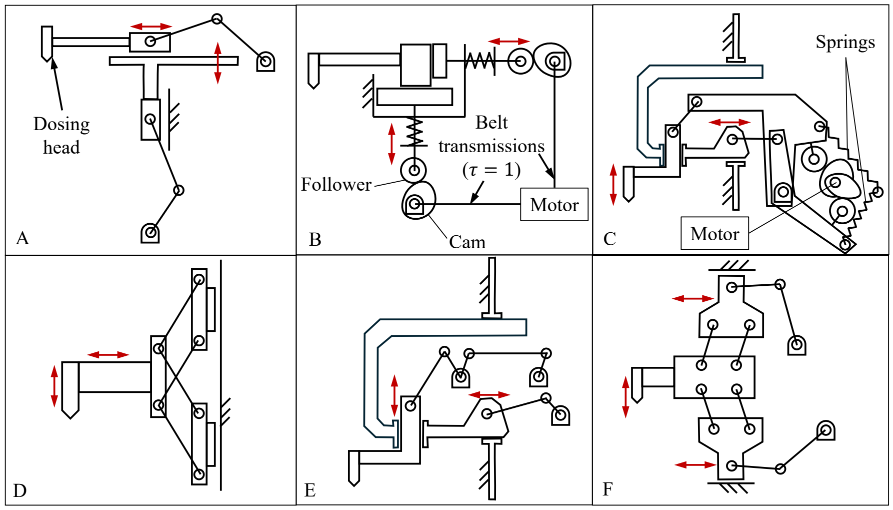

Fig. 1: Different design solutions. For simplicity, the mechanism that moves the syringes is not represented. All solutions have two Degrees-of-Freedom (DoFs), except B and C, which have only one DoF; the DH moves in the vertical plane.

2 Design approach

Our design approach comprises three steps: the definition of design objectives and constraints, the conceptual design of different solutions, and the sizing of components and final design [4]. The alternatives were defined taking inspiration from available designs and patents, together with industrial design experience. We identified six main solutions (Fig. 1); for each solution and for each design objective, we assigned (Tab. 1) a rating from 0 ("negative") to 4 ("very positive"). The six solutions only differ for the technologies used to move the DH, whereas the syringe motion is always realized by a SCL. The structure of each solution and the corresponding advantages are described in the following.

A) The DH is moved by two SCLs actuated by two rotary motors fixed to the frame, thus reducing the moving masses and increasing dynamic performances. However, the mechanism is separated from the product by a single bellow, which deflects laterally, which reduces its fatigue life.
B) The DH motion system comprises a single rotary motor and two cam-follower mechanisms actuated through belt transmissions. This solution uses only one bellow, thus presenting the same issue as solution A. Also, cams require abundant lubrication and are not recommended for pharmaceutical machines.
C) One rotary motor actuates two cam-follower mechanisms coupled with two linkages moving the DH. Two bellows are used here, each deforming only along its main axis, making this solution easily washable. On the other hand, the use of cams raises the same issues as solution B.

D) Two linear motors actuate two sliders that are connected with the DH through two FBPs. This solution still has issues in terms of leakages and washability. Also, linear motors are more expensive than rotary ones.
E) This solution has two rotary motors, each actuating a SCL, and a FBP used as a transmission. The use of two bellows only deforming along their axial directions make the group easy to wash. Also, the overall mechanism is simple, compact, and fast.
F) Two rotary motors actuate two FBPs and two SCLs. The group has many components, thus increasing dimensions and decreasing simplicity. Also, separating the mechanism from the product can be problematic, reducing washability.

The highest total score is achieved by solution E, which features three main linkages (Fig. 2): a SCL for the motion of the pistons in the syringes (not shown in Figs. 1 and 2), a SCL coupled with a FBP for the vertical motion, and a SCL for the horizontal motion. This solution has three rotary motors: two are fixed to the frame (motors 1 and 2 in Fig. 2), thus reducing the moving inertias and increasing the maximum allowable velocities and accelerations, one (actuating the syringe piston motion) moves with the DH. The SCL for the DH vertical motion is not directly connected to motor 2 due to lack of space; a FBP is thus used as a homokinetic transmission. Using several SCLs simplifies sizing, as their kinematic and dynamic analyses can be analytically solved, and then the solution method (implemented, in our case, by a script) can be applied for all linkages just by changing design parameters. To follow the assigned trajectory, motors act in parallel: the horizontal motion is regulated by motor 1, while motor 2 compensates for the induced change in the vertical position of the DH so that the latter remains at a constant height while motor 1 rotates. From the dynamic point of view, motors act in parallel to compensate for the inertial forces of the DH syringes and provide the torques required for the desired motion. Despite the complication of motor synchronization, this solution was chosen over the others due to its high speed, simplicity, washability, and compactness (and thus, low weight of the moving parts). In particular, solutions B and C are avoided due to the lubrication required by cams. Solution F is characterized by several moving parts that are relatively large and heavy: this would negatively impact the operating speed of the mechanism. Solution E wins over solutions A and D in terms of washability, due to the dedicated bellows undergoing purely axial deformations.

	A	**B**	**C**	**D**	**E**	**F**
Speed	3	3	3	3	3	2
Lubricant leakage	2	1	1	2	4	3
Lubrication efficiency	3	1	1	2	3	2
Washability	1	1	4	2	4	1
Simplicity	3	1	3	3	3	2
Dimensions	3	2	2	3	3	2
Total	15	9	14	15	**20**	12

Table 1: Scores for each design solution in Fig. 1, according to the design objectives.

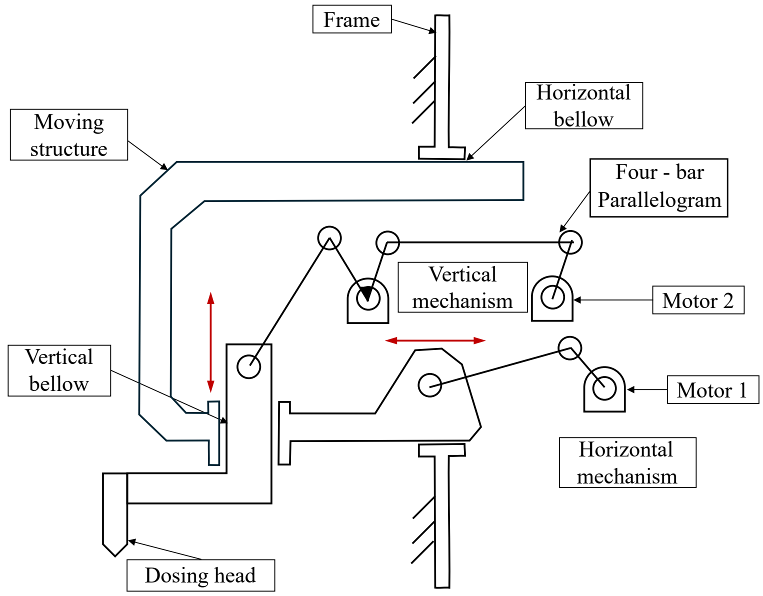

Fig. 2: Schematic of the solution adopted, corresponding to Fig. 1 E.

During the dimensional design stage, we determine the optimal solution in terms of link dimensions, transmission ratio, and motion law. The dimensions of the links are optimized to avoid singular configurations, high transmission angles, and excessively high accelerations, while minimizing the transmission ratio throughout the working range. This way, the unavoidable errors in motor control have a reduced effect on the piston stroke. Finally, we solve the dynamics, obtaining the forces and torques exchanged between the links; from this, we find the overall machine dimensions and the sizing of all components (including the gearboxes and the motors).

3 Dosing unit design

Figure 3 shows the global schematic and the CAD model of the dosing unit proposed in this paper; in particular, Fig. 3b shows the bellows, the syringes, the vacuum system, and the external housing. In Fig. 4, the CAD models of the mechanisms for the syringe motion, the horizontal motion, and the vertical motion are shown in yellow, red, and blue, respectively. The mechanism presents 12 links (each one denoted as $i = 0, 1, \cdots, 11$), 12 revolute joints, and 3 prismatic joints; it thus has 3 DoFs according to Grübler's equation (2 for the DH translation and 1 for moving the syringes). In particular, the frame is member 0, the SCL for the horizontal motion is defined by members $0-1-2-3$, members $0-4-5-6$ define the FBP, members $0-6-7-8$ define the SCL for the horizontal motion, and members $8-9-10-11$

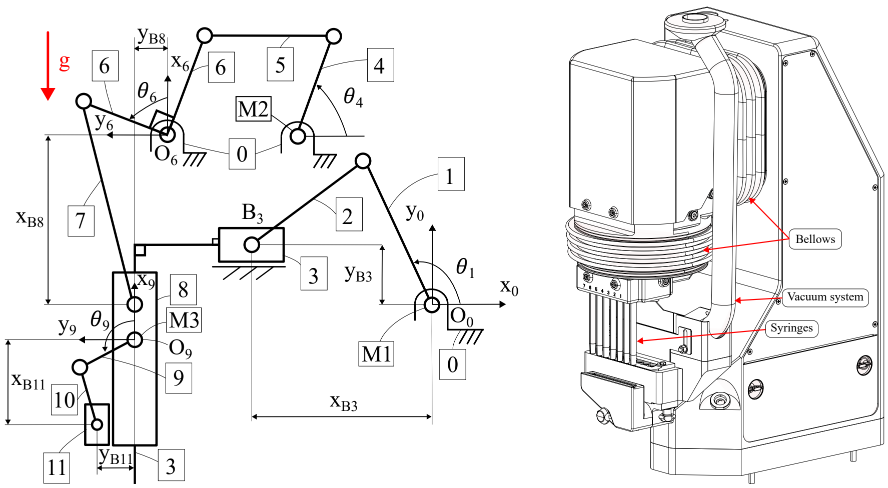

Fig. 3: Global schematic (a) and CAD view of the exterior (b) of the dosing unit. Member 6 is L-shaped, coupled to the frame at O_6, and connecting links 5 and 7.

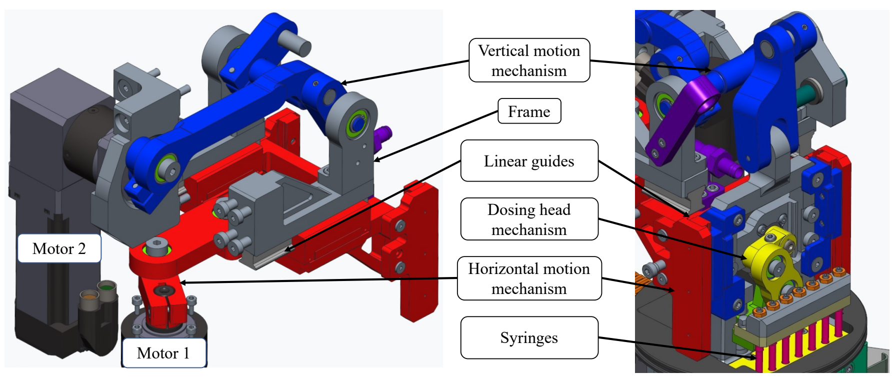

Fig. 4: CAD views of the internal components of the dosing unit.

define the SCL for the syringe motion in the DH. M1, M2, and M3 are the three motors: M1 controls the coordinate x_{B3}, M1 and M2 together control x_{B8}, while M3 controls x_{B11}. Since the vertical motion is controlled by motors M1 and M2, x_{B8} is a function of θ_1 and θ_4.

We first perform the kinematic analysis through the iterative process described in Sec. 3.1 to determine the optimal link lengths, the transmission ratio τ from motor 3 to member 11, and the optimal end-effector trajectory.

Critical components, such as the crank of each linkage (members 1, 4, and 9), the connecting rod of the FBP (member 5), and the linear guides are dimensioned using FEA, since they have a complex, non-standard design. In particular, the cranks are connected to their shafts using both a parallel key and a clamping system regulated by a screw to obtain the desired coupling pressure. This is recommended when alternating motion occurs; since the screw tends to unscrew over time due to vibrations, the key acts as a failsafe system, while an operator periodically tightens the screw. FEA is also used to choose the angular position of the key and the preload of the screw to have uniform coupling pressure and to avoid yielding.

3.1 Kinematic and dynamic analysis

The kinematic and dynamic analyses of the SCLs are the same for all three linkages. We consider a generic SCL with an offset, where the sliders (links 3, 8, and 11) move along an axis at a distance $y_{Bi}(t)$ from the crank pivot O_i. This value is not constant in the linkage for the vertical motion (see y_{B8}) but varies depending on the motion of slider 3. The lengths and the angular positions of the links are denoted as l_i and θ_i. Note that, for the FBP connecting M2 with the SCL for the vertical motion, $l_4 = l_6$, $\theta_4 = \theta_6$ and $\theta_5 = 0$. In particular, member 6 acts as an output crank for the FBP and an input crank for the SCL. The internal angle at O_6 is optimized to minimize the exchanged forces and avoid singularities. The optimal value was found to be 90°.

For each linkage, the loop-closure equations are solved to find the unknown angles through the Newton-Raphson method, knowing the motion of the sliders, namely, the coordinates x_{Bi} and y_{Bi} ($i = 3, 8, 11$). First, we solve the SCL for the syringe motion, then the linkages for the vertical and horizontal motions of the DH. Differentiating the closure equations with respect to time, we find the angular velocities and accelerations $\dot{\theta}_i$ and $\ddot{\theta}_i$. In the optimization procedure (Sec. 3.2), the transmission angle $\pi - \theta_{10}$ of the DH slider is minimized to reduce the forces required to move the pistons.

In the dynamic model, friction is disregarded; therefore, a safety factor is applied to increase the motor torques computed for sizing. From the mass m_i of each member and the corresponding inertia J_{Gi}, the dynamics equations are solved, knowing the positions, velocities and accelerations from the kinematic analysis. We are considering the general case of a non-inertial system, since the SLC in the DH is not mounted on the frame. Thus, the formula for the inertial force $\mathbf{F}_{Ii}$ on the i-th member contains an extra acceleration term $\mathbf{a}_{ei}$:

$$\mathbf{F}_{Ii} = m_i \left(\frac{d^2}{dt^2} \begin{bmatrix} x_{Gi} \\ y_{Gi} \end{bmatrix} + \mathbf{a}_{ei} \right) \tag{1}$$

The dynamic equations also depend on the external forces and moments ($\mathbf{F}_{ei}$, M_{ei}), the gravitational forces ($\mathbf{F}_{Gi}$), the reaction forces and torques ($\mathbf{F}_{Ri,j}$, $M_{Ri,j}$), and the inertia moments (M_{Ii}).

Considering the torque and force equilibrium of each member, we find 11 linear equations in 11 variables. We first consider the DH unit and calculate the torque on

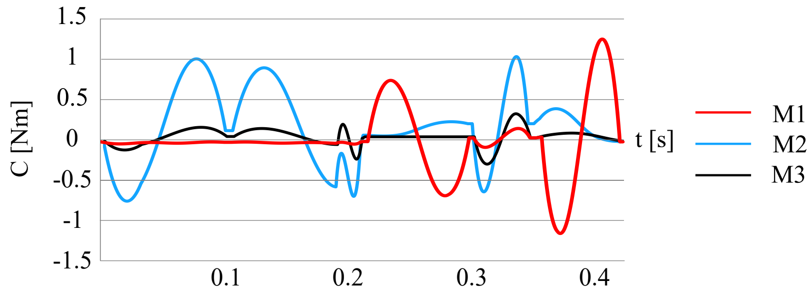

Fig. 5: Torques M1, M2 and M3 as functions of time, with the machine operating at its rated speed of 140 cycles/minute.

M3, with $\mathbf{a}_{e9} = \begin{bmatrix} \ddot{x}_{B8} \\ \ddot{y}_{B8} \end{bmatrix}$ in Eq. (1), and M_{e11} and $\mathbf{F}_{e11}$ equal to zero[1]. To obtain the torque on M2, we solve again the same system with $\mathbf{a}_{ei} = \mathbf{0}$, $\mathbf{F}_{e8} = \mathbf{F}_{R8,9} + \mathbf{F}_{R8,11}$ and $M_{e8} = M_{R8,9} + M_{R8,11}$. Finally, the torque on M1 is obtained considering $\mathbf{a}_{ei} = \mathbf{0}$, $\mathbf{F}_{e3} = \mathbf{F}_{R3,8}$ and $M_{e3} = M_{R3,8}$. The torques on M1, M2, and M3 as functions of time (over one machine cycle) are shown in Fig. 5.

3.2 Optimization

The link dimensions are selected through an iterative process implemented in MATLAB. The optimal dimensions ensure at the same time that the linkages have no singularities in their working range, a small transmission angle (to reduce the exchanged forces), and minimal overall dimensions.

The transmission ratio τ (Fig. 6) of the DH is minimized to reduce the error in the quantity of product to be dosed. τ is the ratio between the slider position x_{B11} and the motor angular position θ_9 [5]. A small value of τ means that the motor can move the slider precisely, since small motor position errors in θ_9 cause smaller errors in x_{B11}. We have $\tau = \tau_{Gb}\tau_{SC}$, where τ_{Gb} is the constant reduction ratio of the gearbox, and τ_{SC} is the variable transmission ratio of the SCL (depending on the crank position). The working range depends on the possible height of the chamber, which in its turn depends on the quantity of product to be dosed. The chamber height is assumed to be between 5 and 30 mm, since heights smaller than 5 mm are rarely used in practice (they would result in too small product quantities). Considering the curve in Fig. 6, the minimum error (for $\tau = 0.042$ mm/°) is achieved at the working limit (chamber height of 5 mm), while the maximum error (for $\tau = 0.051$ mm/°) is when the chamber height is at 16.5 mm. We chose an encoder with a constant resolution of 0.167° and set a maximum admissible error of 1.5% in the piston position. Multiplying the resolver resolution, which is the maximum angular error, by the transmission ratio,

---

[1] The compaction and expulsion force on the pistons is negligible according to industrial experience.

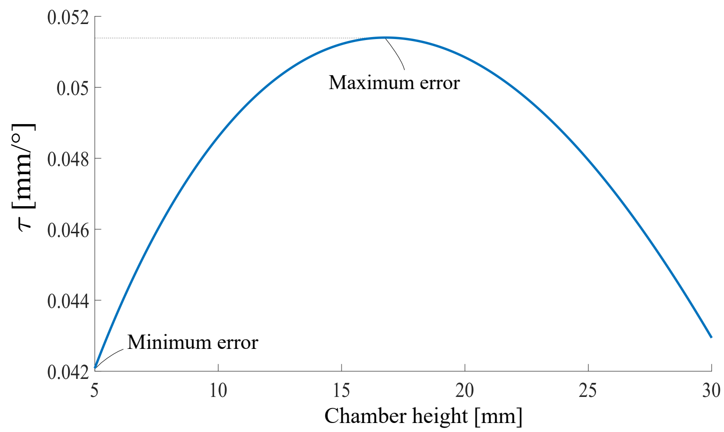

Fig. 6: The overall transmission ratio τ as a function of the chamber height. Since $\tau = \tau_{Gb}\tau_{SC}$ and τ_{Gb} is constant, the plot for τ_{SC} is the same (up to a scale factor).

and considering a chamber height from 0 to 30 mm, we find that for small dosing quantities (and thus small chamber heights), the encoder resolution would not be sufficient, leading to poor dosing precision. However, since a chamber smaller than 5 mm is outside the working area, the selected encoder is deemed appropriate. The final link dimensions are modified until τ is minimized, respecting the housing dimensions. The gearbox selected has a reduction ratio $\tau_{Gb} = 1/10$, to avoid a multi-stage gearbox, which would increase the dimension and weight of the moving parts. The project of the motor controller is not detailed during this work, and its error is considered constant. We consider the transmission ratio to be a constant gain in the control chain.

The dynamics of each mechanism is solved iteratively, too. The inertial characteristics of the links, such as m_i, J_{Gi}, and the position of the CoM G_i, are optimized to minimize inertia forces. The trajectory is modified to be smooth and reduce acceleration peaks. In particular, the dosing chamber is created slowly, with the constraint that the pistons must be raised before the DH syringes enter the tank.

The final parameters of links, gearboxes, and motors are summarized in Tabs. 2 and 3. The positions of the CoMs are not provided for brevity.

Link	1	2	3	4	5	6, 6’	7	8	9	10	11
l_i [mm]	35	80	/	28	170	28, 35	85	/	27	32	/
y_{Bi} [mm]	/	/	29	/	/	/	/	32	/	/	12.5
m_i [kg]	0.10	0.20	3.60	0.09	0.25	0.11	0.20	3.60	0.06	0.07	0.80
J_{Gi} [kg mm^2]	18.5	170	/	34	/	39	376	/	45	22	/

Table 2: Optimized parameters of the dosing unit. l_6 refers to the length of the FBP output crank, while $l_{6'}$ to the SCL crank; the mass and inertia are for the whole link 6-6’. The vertical distance from O_0 to O_6 (175 mm) is not included in the table.

Motor/gearbox n.	**1**	**2**	**3**
J_{Mi} [kg cm^2]	0.38	0.38	0.03
$C_{M,RMS,i}$ [Nm]	0.38	0.51	0.11
$C_{M,Max,i}$ [Nm]	4	4	1
τ_{Gb}	1/10	1/10	1/10
J_{Gbi} [kg cm^2]	0.08	0.18	0.03
η_{Gbi}	0.96	0.94	0.94

Table 3: Parameters of the motors and their gearboxes; J_{Mi} and J_{Gbi} are their inertias, $C_{M,RMS,i}$ and $C_{M,max,i}$ are the motor torque limits, and η_{Gbi} is the gearbox efficiency.

4 Conclusions

This study presented the design and modeling of a dosing unit for pellets in an automatic capsule-filling machine, focusing on design objectives such as high speed, zero leakage, low lubrication, washability, architecture simplicity, and reduced dimensions. The proposed design solution comprises three rotary motors, three slider-crank linkages, and one four-bar parallelogram. Dedicated rubber bellows separate the pellets from the linkages, reducing the risk of contamination and ensuring washability. A kinematic and dynamic model of the dosing unit was used to optimize the sizing procedure, and FEA simulations were conducted to analyze critical components. A multibody model was used to validate the numerical model. Future work will include prototyping the dosing unit and performing a vibrational analysis, to identify and mitigate possible failures [6].

References

1. Haleem, R. M., Salem, M. Y., Fatahallah, F. A., and Abdelfattah, L. E., 2015. "Quality in the pharmaceutical industry–a literature review". *Saudi pharmaceutical journal,* **23**(5), pp. 463–469. doi:10.1016/j.jsps.2013.11.004.
2. Magnani, P. L., and Ruggeri, G., 1986. *Meccanismi per macchine automatiche*. UTET, Collezione di ingegneria meccanica.
3. Derby, S. J., 2004. *Design of automatic machinery*. CRC Press. doi:10.1201/9781420030846.
4. Pahl, G., Beitz, W., Feldhusen, J., and Grote, K. H., 2007. *Engineering design: a systematic approach*. doi:10.1007/978-1-84628-319-2.
5. Kolovsky, M. Z., Evgrafov, A., Semenov, Y. A., and Slousch, A., 2012. *Advanced theory of mechanisms and machines*. Springer Science & Business Media. doi:10.1007/978-3-540-46516-4.
6. Zaccaria, F., Quarta, E., Badini, S., and Carricato, M., 2022. "Optimal design for vibration mitigation of a planar parallel mechanism for a fast automatic machine". *Machines,* **10**(9), p. 770. doi:10.3390/machines10090770.